Over 1-Watt Analog RoF Signal Transmission Using a 1-km Hollow-Core Photonic Bandgap Fiber

Kai Murakami[1], Souya Sugiura[1], Hironori Yamaji[1], Motoharu Matsuura[1,2], Takeshi Takagi[3], and Kazunori Mukasa[3]

[1] University of Electro-Communications, 1-5-1 Chofugaoka, Chofu, Tokyo, 182-8585, Japan
[2] Keio University, 3-14-1 Hiyoshi, Kouhoku, Yokohama, Kanagawa, 223-8522, Japan
[3] Furukawa Electric Co. Ltd., 20-16 Nobono, Kameyana, Mie, 519-0292, Japan
Author e-mail address: m.matsuura@uec.ac.jp

Abstract: We demonstrate analog RoF transmission with signal power exceeding 1-Watt using a hollow-core photonic bandgap fiber. Due to the low nonlinearity, superior transmission performance was obtained in single- and four-channel transmission compared to silica-core fibers.

1. Introduction

Recently, hollow-core fibers (HCFs) have attracted much attention because of their features such as low nonlinearity and low latency, which are difficult to achieve with solid silica-core fibers [1]-[8]. Until now, various kinds of HCFs such as photonic bandgap fibers (PBGFs) [1]-[4] and nested anti-resonant nodeless fibers (NANFs) [5]-[8] have been reported. One attractive application area to take advantage of the low latency is radio-over-fiber (RoF) links in future mobile networks [9]. In particular, analog-RoF (A-RoF), which transmits radio-frequency (RF) data signals by directly intensity modulation, is advantageous for transmitting higher-frequency mobile data signals and simplifying remote antenna unit (RAU) configuration. In addition to the broad bandwidth and low loss of conventional silica-core fibers, it can transmit mobile data signals with a lower latency, making it an effective technology for future mobile communication systems.

In such networks, higher frequencies of mobile data signals will be essential to achieve higher-capacity mobile data communications. This will lead to a rapid shift to smaller cell sizes and the need for more RAUs. Therefore, it is important to increase the power and channels of A-RoF data signals and deliver the signals to a larger number of RAUs for future mobile networks. For this application, HCFs are suitable as A-RoF links due to their low nonlinearity and high-power transmission tolerance. Indeed, an experiment with optical power transmission exceeding 1 kW using a 1 km HCF have been reported [10]. Furthermore, by transmitting high-power feed light along with A-RoF data signals using optical fibers, RAUs can be also driven without the need for any external power supply system [11]-[13]. Until now, some results have been reported on A-RoF transmission and high-power transmission experiments using NANFs [9],[10] and ingle-channel digital signal transmission using PBGFs [14], there have been no report on high-power, multichannel A-RoF transmission experiments using HCFs, to the best of our knowledge.

In this work, we demonstrate single- and four-channel A-RoF transmissions with the signal power exceeding 1 W using a 1-km PBGF-based HCF. To clarify the effectiveness, a comparative evaluation of transmission performance is performed using solid-core, standard single-mode fibers (SMFs) with the same length. As a result, we have shown that the single- and four-channel A-RoF transmissions using the HCF achieve high transmission performance even if the signal power input to the HCF exceeds 32 dBm.

2. Experimental Setup

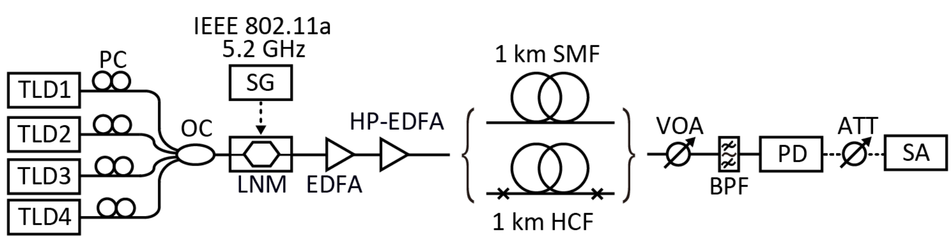

Fig. 1. Experimental setup for high-power A-RoF transmission. TLD: Tunable Laser-Diode, PC: Polarization Controller, OC: Optical Coupler, SG: Signal Generator, LNM: $LiNbO_3$ modulator, EDFA: Erbium Doped Fiber Amplifier, HP-EDFA: High-Power EDFA, SMF: Single-Mode Fiber, HCF: Hollow-Core Fiber, VOA: Variable Optical Attenuator, BPF: Band-Pass Filter, PD: Photo-Diode, ATT: electrical Attenuator, SA: Signal Analyzer.

Figure 1 shows the experimental setup for high-power A-RoF transmission. As seed light sources, four tunable laser-diodes (TLDs) with a spectral linewidth of 70 kHz were used. For these wavelengths, the wavelength of TLD3 was fixed at 1558.98 nm, and the other wavelengths were set to 50 GHz and 100 GHz channel spacings. The state of polarization of each seed light was adjusted by polarization controllers (PCs) at the output of the TLDs, and then combined by an optical coupler (OC) before input to a $LiNbO_3$ modulator (LNM) for the external modulation. The electrical data signal was based on the IEEE 802.11a standard using 64-quadrature amplitude modulation (64-QAM) and orthogonal frequency-division multiplexing (OFDM) format with a carrier-frequency of 5.2 GHz, and was generated using a signal generator (SG). To generate multichannel A-RoF data signals, the electrical data signal was input directly to the LNM. A two-stage erbium-doped fiber amplifier (EDFA) was used to generate high-power A-RoF data signals. A common EDFA was deployed in the first stage, and a high-power EDFA (HP-EDFA) with an output power of more than 30 dBm was deployed in the second stage. The following two fiber links were used as test fibers. One is a standard single-mode fiber (SMF). The other is a hollow-core fiber (HCF) composed of a photonic bandgap structure, called Perturbed Resonance for Increased Single Modedness (PRISM), which has six cores next to the center core corresponding to 19 cells [4]. The transmission loss of the fiber was approximately 3.11 dB/km@1550 nm, and the lowest loss wavelength band existed in the wavelength band centered around 1550 nm and exceeding 20 nm. The chromatic dispersion was approximately 50 ps/nm. SMFs were fusion spliced to both ends of the fiber, and the connection loss per end was approximately 1.1 dB. The fiber length was 1 km for both the SMF and the HCF, and they were connected to the transmission system with connectors at both ends. After transmission, a variable optical attenuator (VOA) was used to reduce the A-RoF data signal power and unify the power input to the PD to 5.5 dBm. The role of the rectangular-shape band-pass filter (BPF) with a 3-dB bandwidth of 0.4 nm was used to select one of the multichannel A-RoF data signals. After converting the selected A-RoF data signal into the electrical signal using a photo-diode (PD), the signal quality was measured using a signal analyzer (SA) while adjusting the input power with an electrical attenuator (ATT), and was quantitatively evaluated with respect to error-vector-magnitude (EVM).

3. Experiments

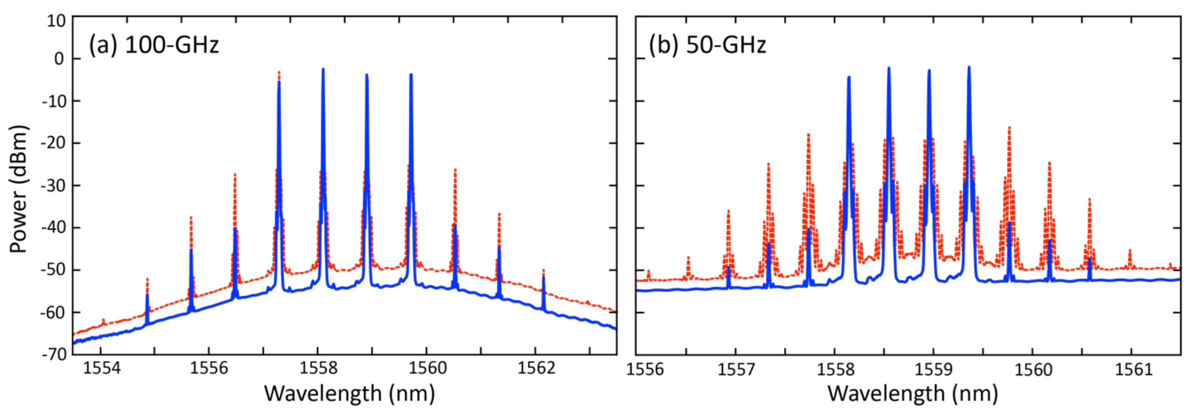

Fig. 2. Output signal spectra of four-channel SMF (red dashed curve) and HCF (blue solid curve) transmissions in cases of (a) 100 GHz and (b) 50 GHz channel spacings.

To observe the nonlinear effect of multichannel transmission, we measured the output four-channel signal spectra with the total 32 dBm injected power into both the SMF and the HCF links. The results are shown in Fig. 2. In the SMF link transmission (red dashed curve), significant spectral components due to four-wave-mixing (FWM) occurred on both sides of the four-channel signal spectra. In particular, more pronounced spectral components were observed in the 50 GHz channel spacing as shown in Fig. 2(b). The peak power difference between the signal and FWM-induced spectra was approximately 15 dB. On the other hands, in the HCF link transmission (blue solid cure), a small amount of the spectral component generated by the FWM was observed. As the same FWM degree was observed in back-to-back where the transmission system was directly connected with a 1 m SMF, we think that this was not caused by the HCF link but by the extra length of the SMF connecting the transmission system. In addition, it was found that the noise level was reduced in the HCF link compared to the SMF link. This is due to the reduction of the signal component power relative to the amplified spontaneous emission (ASE) noise due to stimulated Brillouin scattering (SBS) in the SMF link. These results indicate that HCF link is advantageous for dense wavelength-division-multiplexing (DWDM) transmission using high-power signals. In the following experiment, the channel spacing was set to 50 GHz for four-channel transmission.

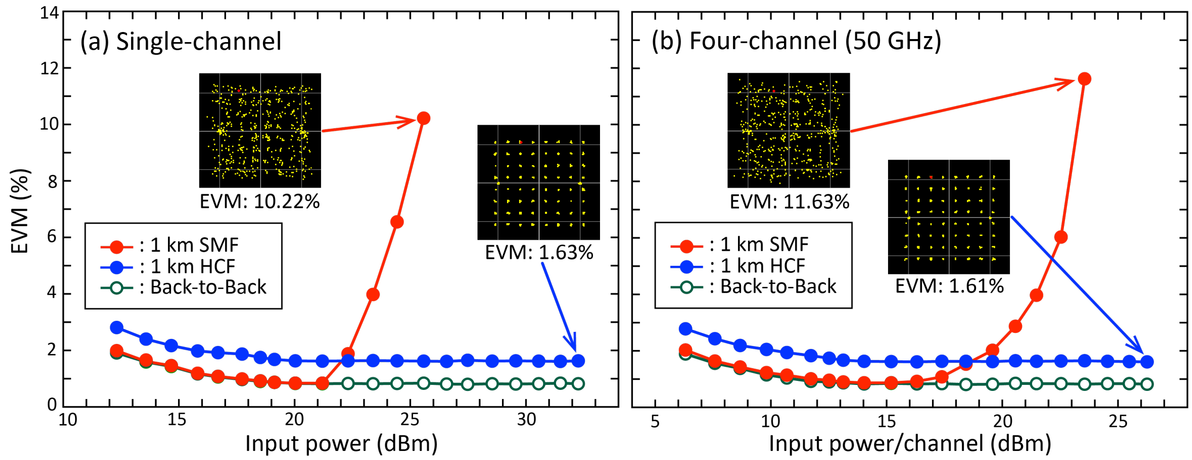

Fig. 3. EVM characteristics as a function of input power in cases of (a) single- and (b) four-channel (50 GHz) transmission. Insets shows constellations of transmitted signals.

The EVM characteristics of the SMF and HCF links as a function of input signal power is shown in Fig. 3. In single-channel transmission as shown in Fig. 3(a), the EVM of the SMF link increased rapidly when the input power exceeded 21 dBm. This was because the input signal power exceeded the SBS threshold of the SMF link. Thereafter, the EVM increased due to the increase in ASE noise caused by the HP-EDFA as the input power increased. On the other hand, the EVM of the HCF link maintained a small EVM even at an input power of 32.26 dBm. Slightly larger EVMs of the HCF link were observed overall compared to the EVMs in the back-to-back and the SMF link at small input power levels. We think this is due to the higher chromatic dispersion and transmission loss of the HCF link.

Figure 3(b) shows the EVM characteristics of the four-channel SMF and HCF transmissions with a channel spacing of 50 GHz as a function of input signal power/channel. In this case, the EVM of the SMF link increased gradually when the input power exceeded 15 dBm. This shows the impact on EVM at smaller input power levels than SBS in the single channel transmission, and is because of the FWM effect induced in the SMF link. Thereafter, the EVM increased slowly due to the synergistic effects of the increased FWM effect and SBS. For the HCF link, the EVM succeeded in achieving high transmission performance even at an input power of 32.26 dBm as well as for single-channel transmission. The obtained results indicate that high transmission performance of the PBGF-based HCF link could be obtained in high-power, multichannel A-RoF signal transmission.

4. Conclusions

We successfully demonstrated high-power A-RoF signal transmission using a hollow-core photonic bandgap fiber. This fiber indicated no EVM penalty even at input signal power up to 32 dBm in cases of single- and four-channel signal transmission. The obtained characteristics greatly exceed those of conventional solid silica-core fibers and would be useful for high-power, multichannel signal transmission in future mobile networks.

Acknowledgements: This work was supported in part by the "Research and Development of Advanced Optical Transmission Technologies for a Green Society" commissioned by the Ministry of Internal Affairs and Communications (MIC) and by the National Institute of Information and Communications Technology (NICT) (07101). This research was conducted at the Keio Future Optical Network Open Lab. The authors also appreciate for the technical supports and discussions of OFS.

References

[1] P. J. Roberts et al., "Ultimate low loss of hollow-core photonic crystal fibres," Opt. Express, **13,** 236-244 (2005).
[2] M. N. Petrovich et al., "Robust single mode hollow core photonic bandgap fiber," Opt. Express, **16,** 4337-4346 (2008).
[3] J. M. Fini et al., "Low-loss hollow-core fibers with improved single-modedness," Opt. Express, **21,** 6233-6242 (2013).
[4] B. Zhu et al., "First demonstration of hollow-core-fiber cable for low latency data transmission", in Proc. OFC 2020, Th4B.3.
[5] A. N. Kolyadin et al., "Light transmission in negative curvature hollow core fiber in extremely high …," Opt. Express, **21,** 9514–9519 (2013).
[6] F. Poletti, "Nested antiresonant nodeless hollow core fiber," Opt. Express, **22,** 23807-23828 (2014).
[7] D. Richardson et al., "Hollow core fibers: Key properties, technology status and telecommunication …," in Porc. OFC 2022, W4E.1.
[8] E. N. Fokoua et al., "Loss in hollow-core optical fibers: mechanisms, scaling rules, and limits," Adv. Opt. Photonics, **15,** 1-85 (2023).
[9] X. Zhang et al., "Low-loss microwave photonics links using hollow core fibers," Light Sci. Appl. **11,** 213 (2022).
[10] H. C. H. Mulvad et al., "Kilowatt-average-power single-mode laser light transmission over …," Nature Photon., **16,** 448-453 (2022).
[11] M. Matsuura, "Bidirectional radio-over-fiber systems using double-clad fibers for optically …," IEEE Photon. J., **7,** Art. no. 7900609 (2015).
[12] M. Matsuura, "Power-over-fiber using double-clad fibers," J. Lightwave Technol., **40,** 3187-3196 (2022).
[13] N. Parkin and A. Lord, "A telecom operator perspective on hollow core fibre," in Proc. ECOC 2023, Tu.C.4.1.
[14] S. Kimura at al., "+30.8 dBm, IM-DD, 32 Gbit/s high power optical transmission with a 4-km photonic …," in Proc. of PSC 2023, Fr2B.6.